ADVANCED LINEAR AND NONLINEAR OPTICS STUDIES USING MAD-NG'S PARAMETRIC DIFFERENTIAL ALGEBRA

L. Deniau, European Organization for Nuclear Research, Geneva, Switzerland

Abstract

Advanced linear and non-linear optics studies require accurate and efficient tools for high-order beam dynamics computations. MAD-NG provides a unique framework combining linear and nonlinear optics modelling, high-order parametric differential map computation through precise automatic differentiation, and Lie-algebraic operations central to nonlinear normal form analysis, all within a unified environment based on the Generalised Truncated Power Series Algebra (GTPSA). These capabilities enable an accurate evaluation of optical functions, chromatic effects, and nonlinear Hamiltonian dynamics. MAD-NG embeds LuaJIT, a high-performance scripting engine, offering automated workflows, symbolic dependencies, and deferred evaluations for efficient lattice design and parametric optimisation. It has been used successfully to improve the LHC beam lifetime at injection (2023) and during collisions (2025) by minimising resonant driving terms. Applied to major projects such as the LHC, HL-LHC, and FCC-ee, MAD-NG demonstrates reliability, scalability, and accuracy for large-scale optics and sensitivity studies while providing a flexible, reproducible, and high-performance environment for modern accelerator modelling and advanced beam dynamics research.

INTRODUCTION

Modern accelerator studies require a consistent description of beam dynamics across linear optics, chromatic effects, and nonlinear dynamics, often under variations of many parameters such as magnet strengths, alignment errors, and RF settings. In practice, this means computing not only optical functions, tunes, and chromaticities, but also their sensitivities and the resonance structure governing beam stability.

Existing tools typically separate these aspects. Tracking codes such as XSuite [1] provide high physical fidelity but limited direct access to sensitivities and high-order structures. Optics codes such as MAD-X [2] manipulate differential maps for analysis and optimisation, but usually through low-order approximations or specialised formalisms that are difficult to extend consistently to high order and large parameter spaces.

MAD-NG [3] addresses this limitation by providing a unified framework in which linear and nonlinear optics, high-order beam dynamics, and parametric studies are described within a single coherent formalism based on differential algebra and the Generalised Truncated Power Series Algebra (GTPSA) [4]. The central object is a parametric differential map from which linear optics, chromatic effects, and nonlinear quantities are obtained consistently. This provides direct access to high-order effects and sensitivities while avoiding repeated perturbations of the lattice and the associated risk of approaching unstable regimes.

PARAMETRIC DIFFERENTIAL MAP FRAMEWORK

In MAD-NG, the central object of the tracking engine is the phase-space propagator

$$z(s) = \mathcal{M}(z_0; \mathbf{p}), \tag{1}$$

where z denotes the phase-space variables and $\mathbf{p}$ a set of machine parameters. The map $\mathcal{M}$ is not constructed as an expanded matrix or tensor a priori, but results from applying the beam-physics functions of the lattice elements to a phase-space DA map, i.e. a set of truncated multivariate Taylor polynomials in the initial variables and selected parameters.

The dynamics is therefore obtained by successive functional application of the element transformations, applied either analytically or, for general elements, through exact element-wise operations and symplectic integration of the Hamiltonian flow. The only approximation is the user-controlled truncation of the GTPSA representation. This allows high-order maps to be computed with the full functional dependence of the physics retained throughout the lattice.

This framework naturally supports parametric studies. Quantities such as strengths, lengths, or misalignments are promoted to DA parameters, so that a single computation provides the local dependence of the optics on these quantities around a chosen reference configuration. The sensitivities and mixed derivatives are then read directly from the coefficients of the same map, without finite differences, repeated tracking, or lattice perturbation.

The same map can also be constructed through Lie-algebraic methods [5]. For instance, for a sextupole,

$$H = H_{\text{drift}} + \frac{k_2}{6}(x^3 - 3xy^2), \tag{2}$$

$$z(s; k_2) = e^{\{\cdot, lH\}}\, z(s_0; k_2), \tag{3}$$

with k_2 treated as a DA parameter. The corresponding map is $\mathcal{M}(\cdot; k_2) = e^{\{\cdot, lH\}}$, implemented in MAD-NG through `exppb`. Tracking and Lie integration thus provide two consistent constructions of the same parametric map.

LINEAR OPTICS AND CHROMATIC SENSITIVITIES

Linear optics quantities are obtained directly from the first-order part of the parametric one-turn map. Twiss parameters, phase advances, and dispersion functions are extracted from the linear normal form of the transfer matrix, while their sensitivities are obtained as multivariate functions of the selected parameters. This gives direct access to quantities such as

$$\frac{\partial Q}{\partial k_1}, \quad \frac{\partial Q'}{\partial k_2}, \quad \frac{\partial^2 Q}{\partial J\,\partial k_1}, \quad \frac{\partial^2 \beta}{\partial k_1\,\partial k_{1s}}, \quad \frac{\partial^2 \mu'}{\partial k_2\,\partial \delta_x^{\text{sext}}}, \tag{4}$$

together with higher-order derivatives when required.

Figure 1 illustrates these capabilities in the ATS optics of the LHC [6]. The first panel shows the reference optics, while the following panels show the derivatives of $\beta_{x,y}$, $D_{x,y}$, and $\mu_{x,y}$ with respect to the horizontal and vertical tune knobs. The β-function sensitivities exhibit large oscillatory patterns correlated with the optics, with amplitudes scaling with the local β values. The dispersion sensitivities show a more structured response, with localised peaks associated with focusing regions and dispersion suppressors, and enhanced amplitudes in the ATS arcs. The phase-advance response is the most directly related to the tune knobs: $\partial\mu/\partial q$ increases monotonically and reaches unity after one turn, while flat regions identify sections where the knobs do not act. In particular, the weak response in the ATS arcs around IP1 and IP5 indicates that these regions do not contribute to the tune variation generated by the selected knobs.

Higher-order chromatic sensitivities are obtained from the same map. Figure 2 shows $\partial\mu'_{x,y}/\partial q_{x,y}$ and $\partial w_{x,y}/\partial q_{x,y}$, corresponding to mixed derivatives such as

$$\frac{\partial \mu'}{\partial q} = \frac{\partial^2 \mu}{\partial q\,\partial \delta}, \qquad \frac{\partial w}{\partial q} = \frac{1}{\beta}\frac{\partial^2 \beta}{\partial q\,\partial \delta} - w\,\frac{1}{\beta}\frac{\partial \beta}{\partial q}. \tag{5}$$

These quantities describe how the tune knobs locally modify the chromatic structure of the optics: $\partial\mu'/\partial q$ gives the redistribution of the chromatic phase advance, while $\partial w/\partial q$ captures the deformation of the chromatic β-functions. Extending the same analysis to second order in the tune knobs reveals significant higher-order contributions, with amplitudes consistent with quadratic parameter dependence. All these sensitivities are obtained within the same parametric framework, without additional user effort beyond increasing the DA orders and extending the requested outputs.

NONLINEAR OPTICS AND NORMAL FORMS

The higher-order components of the map encode the nonlinear dynamics. These maps are analysed in MAD-NG through Lie-algebraic normal forms [7, 8]. The one-turn map is factorised as

$$\mathscr{M} = \mathscr{A} \circ \mathscr{R} \circ \mathscr{A}^{-1}, \tag{6}$$

where $\mathscr{R}$ is the normal form and $\mathscr{A}$ the normalising transformation. The map $\mathscr{R}$ is expressed in terms of invariants and phase advances and provides direct access to amplitude detuning and other nonlinear invariants, while $\mathscr{A}$ contains the geometric information required to reconstruct the full phase-space dynamics.

Anharmonicities are obtained from the nonlinear terms of $\mathscr{R}$, while hamiltonian terms (HTs) and resonance driving terms (RDTs) are obtained from the nonlinear terms of $\mathscr{A}$ in the phasor basis. Because the underlying map is parametric,

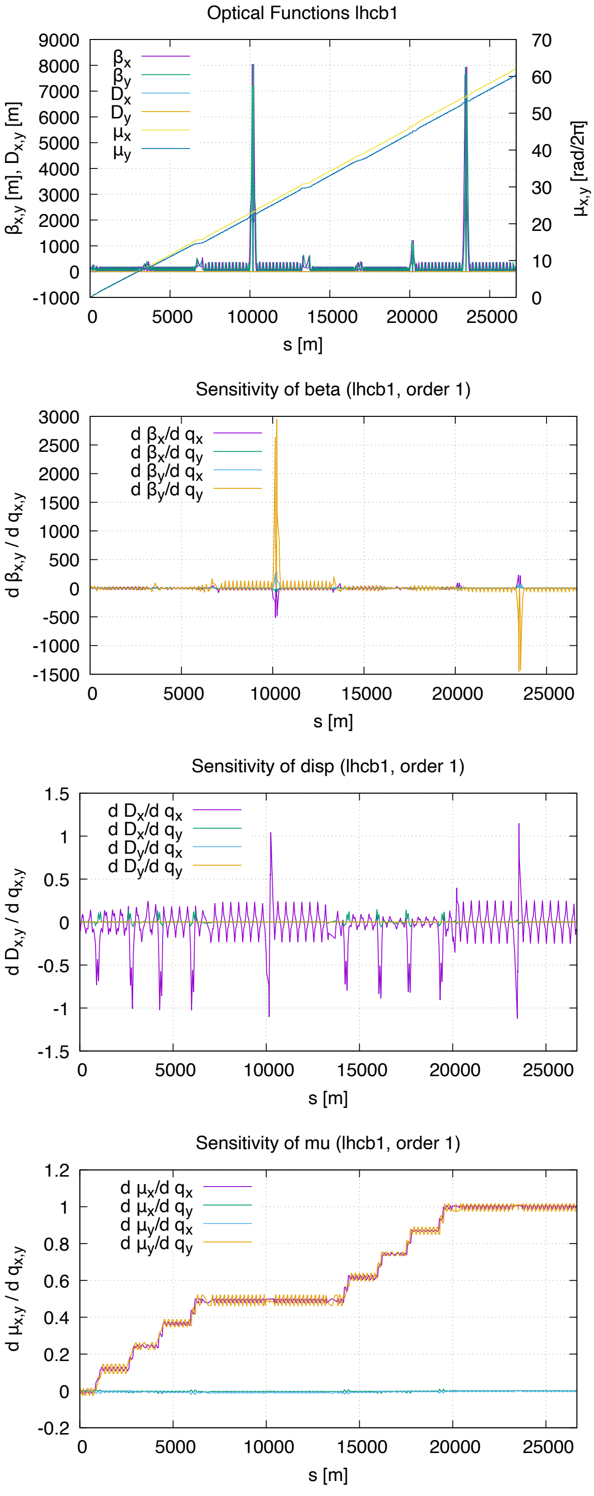

Figure 1: ATS optics of the LHC and its first-order sensitivity to the tune knobs dq_x and dq_y. From top to bottom: reference optics showing β_x, β_y, D_x, D_y, and μ_x, μ_y versus s, followed by the sensitivities of $\beta_{x,y}$, $D_{x,y}$, and $\mu_{x,y}$ to the tune knobs. The phase response integrates to unity, i.e. one unit of knob produces one unit of tune shift.

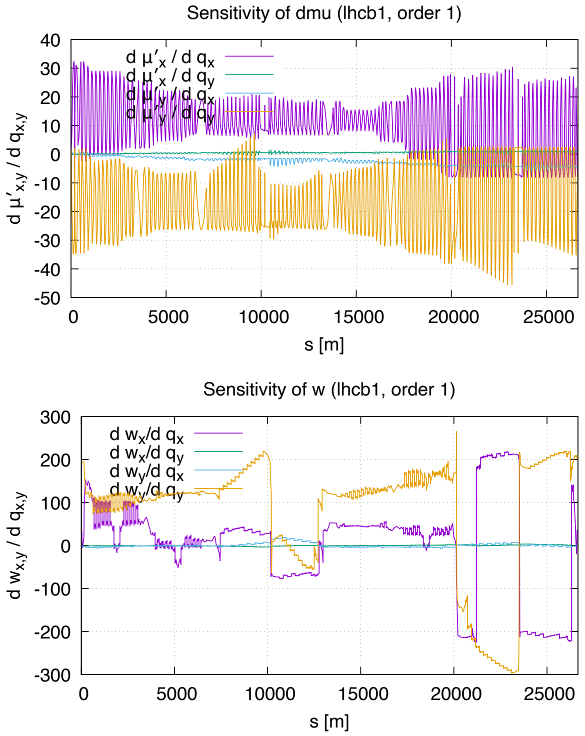

Figure 2: Higher-order sensitivity of the ATS optics to the tune knobs dq_x and dq_y. The panels show $\partial\mu'_{x,y}/\partial q_{x,y}$ and $\partial w_{x,y}/\partial q_{x,y}$, extending the first-order responses of Fig. 1.

the HTs and RDTs are themselves functions of the machine parameters, so derivatives such as

$$\frac{\partial f_{jklm}}{\partial k_n}, \qquad \frac{\partial f_{jklm}}{\partial \delta_x}, \qquad \frac{\partial f_{jklm}}{\partial q_x}, \tag{7}$$

are obtained analytically from the same parametric map, without additional tracking or numerical approximation.

Figure 3 shows the octupolar RDTs of the HL-LHC injection optics together with the parametric $4Q_x$ RDTs. The upper plot gives the spatial distribution of the dominant octupolar RDTs along the ring and highlights the localisation of the nonlinear driving terms in the lattice, in particular around IP1 and IP5. The lower plot shows the nominal $4Q_x$ RDT together with its first- and second-order dependence on the strengths of the two sextupole families in arc 45. The first-order terms quantify the linear sensitivity of the resonance to each family, while the smaller but visible second-order terms reveal a non-trivial quadratic interplay between the two control knobs. The resonance structure and its sensitivities are therefore obtained within the same map, enabling direct optimisation of selected resonances while preserving the global optics.

PARAMETRIC OPTIMISATION

A key consequence of the parametric differential algebra approach is that sensitivities are obtained as part of the map construction. No lattice perturbation or repeated computation is required to evaluate parameter variations, provided the element models remain well-defined over the parameter

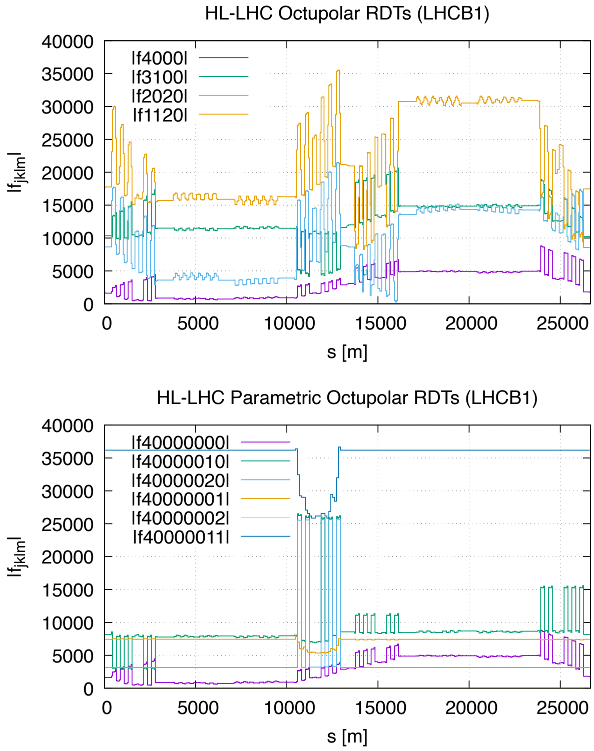

Figure 3: Octupolar RDTs (top) and parametric $4Q_x$ RDTs (bottom) of the HL-LHC injection optics. The lower plots show the first- and second-order dependence on the strengths of the two sextupole families in arc 45, obtained from the same parametric map.

range. In MAD-NG, the Jacobians required by matching and the many optimisation algorithms available are therefore extracted directly from the parametric map, avoiding the numerical noise inherent to finite-difference methods.

This is particularly effective for nonlinear optics optimisation in the LHC, where many knobs and constraints must be handled simultaneously. By treating magnet strengths as DA parameters, derivatives of optical functions, tunes, chromaticities, and RDTs with respect to all selected knobs are obtained in a single computation and can be used directly by the `match` command. This approach contributed to the reduction of resonance driving terms at injection and during collisions, with significant gains in beam lifetime [9–19].

CONCLUSION

Parametric differential algebra thus provides a unified framework for linear and nonlinear optics studies. By representing beam dynamics through high-order multivariate maps, MAD-NG gives direct access to optical functions, chromatic sensitivities, nonlinear invariants, and resonance driving terms within a single formalism, i.e. a single Twiss command, making it a powerful tool for modern accelerator design, modelling, and optimisation.

REFERENCES

[1] G. Iadarola *et al.*, "Xsuite: An Integrated Beam Physics Simulation Framework", in *Proc. HB'23*, Geneva, Switzerland, Oct. 2023, pp. 73–80. doi:10.18429/JACoW-HB2023-TUA2I1

[2] MAD-X project, "Methodical Accelerator Design," https://cern.ch/madx

[3] L. Deniau, "MAD-NG, a standalone multiplatform tool for linear and non-linear optics design and optimisation", in *Proc. ICAP'24*, Oct. 2024. doi:10.48550/arXiv.2412.16006

[4] L. Deniau and C. I. Tomoiaga, "Generalised Truncated Power Series Algebra for Fast Particle Accelerator Transport Maps", in *Proc. IPAC'15*, Richmond, VA, USA, May 2015, pp. 374–377. doi:10.18429/JACoW-IPAC2015-MOPJE039

[5] L. Deniau, "MAD-NG, a standalone multi-platform tool for linear and non-linear optics design and optimisation", ATS Seminar, CERN, Meyrin, Switzerland, Dec. 4, 2025.

[6] S. Fartoukh, "Achromatic telescopic squeezing scheme and application to the LHC and its luminosity upgrade", *Phys. Rev. Spec. Top. Accel. Beams*, vol. 16, p. 111002, Nov. 2013. doi:10.1103/PhysRevSTAB.16.111002

[7] E. Forest, *Beam Dynamics: A New Attitude and Framework*, 1998, CRC Press.

[8] E. Forest, *From Tracking Code to Analysis: Generalised Courant-Snyder Theory for Any Accelerator Model*, Springer, 2016.

[9] L. Deniau, S. Kostoglou, E. H. Maclean, K. Paraschou, T. H. B. Persson, and R. Tomás García, "Optimizing Resonance Driving Terms Using MAD-NG Parametric Maps", in *Proc. HB'23*, Geneva, Switzerland, Oct. 2023, pp. 483–486. doi:10.18429/JACoW-HB2023-THBP15

[10] K. Paraschou *et al.*, "Emittance Growth From Electron Clouds Forming in the LHC Arc Quadrupoles", in *Proc. HB'23*, Geneva, Switzerland, Oct. 2023, pp. 487–490. doi:10.18429/JACoW-HB2023-THBP16

[11] S. Horney *et al.*, "Recap of RDTs between 2022 and 2023 optics," presented at the LNO/OMC Meeting on the LHC Re-start Up and Other Topics, CERN, Geneva, Switzerland, Aug. 24, 2023. https://indico.cern.ch/event/1318103/

[12] E. Manosperti, L. Deniau, A. Pastushenko, and R. Tomas, "MAD-NG for final focus design", in *Proc. IPAC'23*, Venice, Italy, May 2023, pp. 818–821. doi:10.18429/JACoW-IPAC2023-MOPL112

[13] R. Tomas *et al.*, "Mitigation of losses at injection protection devices in the CERN LHC", in *Proc. IPAC'23*, Venice, Italy, May 2023, pp. 547–550. doi:10.18429/JACoW-IPAC2023-MOPL019

[14] R. Tomás *et al.*, "Optics for Landau damping with minimized octupolar resonances in the LHC", *J. Instrum.*, vol. 19, no. 05, p. T05010, May 2024. doi:10.1088/1748-0221/19/05/T05010

[15] S. Horney *et al.*, "Sextupole RDTs in the LHC at injection and in the ramp", in *Proc. IPAC'24*, Nashville, TN, USA, May 2024, pp. 71–74. doi:10.18429/JACoW-IPAC2024-MOPC13

[16] S. Horney *et al.*, "Correction of Long-Range Beam-Beam Driven Normal Sextupolar Resonance Driving Terms", in *Proc. IPAC'25*, Taipei, Taiwan, Jun. 2025, pp. 322–325. doi:10.18429/JACoW-IPAC2025-MOPM019

[17] S. Horney *et al.*, "Investigation of octupolar resonances in the LHC", in *Proc. IPAC'25*, Taipei, Taiwan, Jun. 2025, pp. 326–329. doi:10.18429/JACoW-IPAC2025-MOPM020

[18] J. Gray *et al.*, "Understanding energy-induced optics distortions in the LHC", presented at the IPAC'26, Deauville, France, May 2026, paper WEP5041, this conference.

[19] J. Gray, C. Caliari, F. Carlier, L. Deniau, A. Oeftiger, and K. Skoufaris, "Deep Lie map networks from single-pass forward differentiation", presented at the IPAC'26, Deauville, France, May 2026, paper WEP5042, this conference.